Environ. Sci. Technol. **2005**, *39,* 181−187

Zinc Adsorption Effects on Arsenite Oxidation Kinetics at the Birnessite−Water Interface

LAURA E. POWER,[†] YUJI ARAI,[†,‡] AND DONALD L. SPARKS*,[†]

Department of Plant and Soil Sciences, University of Delaware, Newark, Delaware 19717-1303, and U.S. Geological Survey, Water Resources Division, 345 Middlefield Road, MS 465, Menlo Park, California 94025

Arsenite is more toxic and mobile than As(V) in soil and sediment environments, and thus it is advantageous to explore factors that enhance oxidation of As(III) to As(V). Previous studies showed that manganese oxides, such as birnessite (δ-MnO_2), directly oxidized As(III). However, these studies did not explore the role that cation adsorption has on As(III) oxidation. Accordingly, the effects of adsorbed and nonadsorbed Zn on arsenite (As(III)) oxidation kinetics at the birnessite−water interface were investigated using batch adsorption experiments (0.1 g L^{-1}; pH 4.5 and 6.0; I = 0.01 M NaCl). Divalent Zn adsorption on synthetic δ-MnO_2 in the absence of As(III) increased with increasing pH and caused positive shifts in electrophoretic mobility values at pH 4−6, indirectly suggesting inner-sphere Zn adsorption mechanisms. Arsenite was readily oxidized on birnessite in the absence of Zn. The initial As(III) oxidation rate constant decreased with increasing pH from 4.5 to 6.0 and initial As(III) concentrations from 100 to 300 μM. Similar pH and initial As(III) concentration effects were observed in systems when Zn was present (i.e., presorbed Zn prior to As(III) addition and simultaneously added Zn−As(III) systems), but As(III) oxidation reactions were suppressed compared to the respective control systems. The suppression was more pronounced when Zn was presorbed on the δ-MnO_2 surfaces as opposed to added simultaneously with As(III). This study provides further understanding of As(III) oxidation reactions on manganese oxide surfaces under environmentally applicable conditions where metals compete for reactive sites.

Introduction

Arsenic often occurs in aquatic/terrestrial environments because of anthropogenic inputs (e.g., use of arsenical pesticides) and weathering of indigenous sources (*1*). Recent regulatory changes lowered the maximum concentration level for total As in drinking water to 10 ppb (*2*). Arsenite (As(III)) and arsenate (As(V)) are the most common inorganic As species in soil−water environments (*1*, *3*). Arsenite is more toxic than As(V) and more mobile in soil and sediment environments because of its neutral, uncharged molecular state ($H_3AsO_3°$) in common soil/sediment pH ranges (e.g., pH 5−8) (*1*). Therefore, groundwater contamination by As(III) leaching is a threat to communities, and effective means to enhance conversion of As(III) to As(V) are needed. Many researchers investigated As(III) oxidation chemistry using one of the most powerful soil oxidants, manganese oxides (*4*−*9*). While most studies showed rapid oxidation of As(III) to As(V) on synthetic birnessite in minutes to hours, there were no significant impacts on As(III) oxidation in lake sediments containing Mn-oxides during the first few reaction hours (*4*). This suggests that the other components in the sediments could have inhibited As(III) oxidation. Arsenite oxidation could be inhibited on natural materials because of (i) competitive adsorption between anions/cations and As(III) on manganese oxides or (ii) As(III) adsorption on redox inactive adsorbents (e.g., Al oxides). Oscarson and co-workers investigated the latter hypothesis using Al-oxide and $CaCO_3$ coated MnO_2 and observed a significant decrease in the As(III) oxidation rate, suggesting the importance of As(III) oxidation inhibitory mechanisms by redox inactive mineral coatings on manganese oxides (*4*).

This study investigated competitive metal−ligand effects on As(III) oxidation at the birnessite−water interface in a binary ion (Zn−As(III)) system using macroscopic approaches. Metals that form inner-sphere surface complexes could lower the As(III) oxidation rate more than those forming outer-sphere complexes at the birnessite−water interface. The primary objective of this study was to assess the impact of nonadsorbed and adsorbed Zn on the As(III) oxidation kinetics at the birnessite−water interface. The following experiments were conducted: (i) electrophoretic mobility (EM) measurements on pristine birnessite and Zn-reacted birnessite; (ii) Zn adsorption on birnessite; (iii) arsenite oxidation kinetics at the birnessite−water interface without Zn addition; and (iv) effects of Zn (i.e., presorbed on birnessite surfaces prior to As(III) addition and simultaneous addition with As(III)) on As(III) oxidation kinetics at the birnessite−water interface.

Experimental Section

Materials. Birnessite (δ-MnO_2) was synthesized by the method outlined by McKenzie (*10*) and freeze-dried. X-ray diffraction analysis showed three diagnostic peaks of birnessite at 0.72, 0.36, and 0.24 nm. The specific total surface area of birnessite was 32.6 ± 0.3 m^2 g^{-1} (BET). The percent of pyrophosphate extractable Mn(III) from the birnessite was 3.24 mol %, determined using published procedures (*11*−*13*). Substantial amounts of Mn(III) are present in the lattice or on external surfaces of the synthetic birnessite (*14*−*17*). The isoelectric point (IEP) of the birnessite surface was determined using the electrophoretic mobility measurement method described below. Extrapolating using a second-order polynomial showed the IEP equal to 1.9, which agreed with values found in other studies (*6*, *18*).

Zinc stock solutions were prepared by dissolving ACS-grade zinc chloride salts ($ZnCl_2$, Baker) in 0.1 M NaCl prepared in deionized water (DDI−H_2O, Milli-Q, Millipore Corp., Bedford, MA). Arsenite stock solutions were freshly prepared by dissolving ACS-grade sodium *m*-arsenite ($NaAsO_2$, Baker) in 0.1 M NaCl solutions, and pH values were immediately adjusted to pH 4.5 or 6.0 using 0.1 to 1 M HCl. The absence of As(V) in the As(III) stock solutions was confirmed using an ammonium molybdenum colormetric method by Cummings et al. (*19*). Stock solutions for oxidation experiments conducted in N_2(g) atmospheres were prepared using boiled, CO_2-free DDI−H_2O at pH 4, and the pH was readjusted to 4.5 or 6.0 with CO_2-free 0.1 M NaOH solutions. Zinc stock solutions used for experiments conducted in the glovebox

* Corresponding author phone: (302)831-2535; fax: (302)831-0605; e-mail: dlsparks@udel.edu.
[†] University of Delaware.
[‡] U.S. Geological Survey.

10.1021/es049922i CCC: $30.25 © 2005 American Chemical Society
Published on Web 12/03/2004

were prepared by dissolving $ZnCl_2$ in boiled, CO_2-free DDI−H_2O at pH 4 in a N_2-filled glovebox.

Electrophoretic Mobility Measurements. Electrophoretic mobility (EM) measurements were conducted to assess the effect of Zn sorption on the charge properties of synthetic birnessite between pH 4.0 and pH 8.0. The measurements were performed on a zeta potential meter (Zetasizer 300Hs Malvern, Southborough MA). The birnessite suspension (supension density: 0.1 g L^{-1}) was prepared in the 0.01 M NaCl background electrolyte solutions. Suspensions were sonified and then hydrated in 0.01 M NaCl solutions for 72 h. The pH of the suspensions was adjusted using a Brinkmann Metrohm 718 Stat Titrino (Metrohm, Switzerland) to values between 4.0 and 8.0 with 0.01 M HCl or NaOH and equilibrated for an additional 12−24 h. Each vessel was stirred at 300 rpm while adjusting the pH. The average particle radius of 25 μm and I = 0.01 M were within the Smoluchowski limits for estimating EM (*20*). Zinc stock solution (0.01 M) was added to reach a final Zn concentration of 10−50 μM in the final volume of 60 mL. The reaction vessels were shaken at 300 rpm for 24 h to reach a steady pH. Once a steady pH was reached, 10 mL of suspensions was injected into the zeta meter for analysis.

Zinc Adsorption Experiments. Zinc adsorption onto birnessite (initial Zn concentrations: $[Zn]_i$ =100 μM, I = 0.01 M NaCl, final volume = 60 mL, birnessite suspension density = 0.1 g L^{-1}) was investigated under $pCO_2 = 10^{-3.5}$ atm (i.e., equilibrated in air) as a function of pH (*4*−*8*). Identical Zn concentrations (i.e., 100 μM) were used in the Zn−As(III) oxidation kinetic experiments described below, and therefore the adsorption data were used to interpret changes in As(III) oxidation via Zn adsorption. The MINEQL+ chemical speciation program predicted that Zn was undersaturated with respect to smithsonite ($ZnCO_3$(s)) and zinc hydroxide ($ZnOH_2$(s)) under these reaction conditions (*21*). Sorption studies were conducted using a batch method. Birnessite was hydrated in 0.01 M NaCl solutions in 125-mL Teflon FDP bottles. The pH of the mineral suspensions was preequilibrated at pH 4−8 using 0.1−1 M HCl. After pre-equilibrating for 24 h, 0.1 M Zn stock solution was added to the birnessite suspensions to reach $[Zn]_i$ = 100 μM, and the pH was re-readjusted. After the pH stabilized, the samples reacted for 24 h (a time when steady-state conditions for Zn sorption were attained) on an end-over shaker at 200 rpm, the pH was measured, and the supernatant was filtered through 0.2-μm Supor-200 filter paper (Pall Corporation, Ann Arbor, MI). The samples were analyzed for total Zn using flame atomic absorption (FAA) spectrometry when $[Zn]_T$ concentration was 100 μM. Samples were analyzed for total Zn and Mn with inductively coupled plasma-atomic emission spectrometry (ICP-AES) for the remaining experiments. The detection limits for total Mn and Zn are approximately 0.2 and 0.1 μM, respectively, and percent relative standard deviation (RSD) values are <0.8 for both elements.

The same experiments were repeated in a N_2-filled glovebox since As(III) oxidation kinetic experiments were also performed in a N_2 atmosphere. The MINEQL+ chemical speciation program predicted similar Zn solution speciation to that in the open-air system described above (*21*). The procedure for these experiments was the same, but all steps were carried out in a N_2-filled glovebox.

Arsenite Oxidation Kinetics. Birnessite was hydrated in 500 mL of 0.01 M NaCl solution in Teflon FDP bottles in a N_2(g) atmosphere. The pH of the mineral suspensions was preequilibrated for 24 h at pH 4.5 or 6.0 using a stirred (300 rpm) PHM290 pH-Stat apparatus. Arsenite stock solutions (0.1 M $NaAsO_2$) were added to reach initial As(III) concentrations of 100 or 300 μM and a final birnessite suspension density of 0.1 g L^{-1} at pH 4.5 and 6.0. This concentration range was used in previous studies (*6*, *9*) and was suitable for the analytical methods used in this study. At increasing time intervals (every 2 min at t = 0−4 min, every 4 min at t = 4−60 min, every 20 min at t = 60−120 min, every 40 min at t =120−240 min, every 60 min at t = 240−420 min, and 1440 min), 10-mL aliquots were removed and filtered using 0.2-μm filters. Filtrates were immediately analyzed for As(V) using the ammonium molybdenum method (*19*). Total As and Mn concentrations were determined using ICP-AES with the detection limit for total As being 0.3 μM. The As(III) concentration was calculated by the difference in concentrations of total and As(V) concentrations. Detection limit and %RSD for the As(V) colorimetric method were approximately 5 μM and <1.9, respectively.

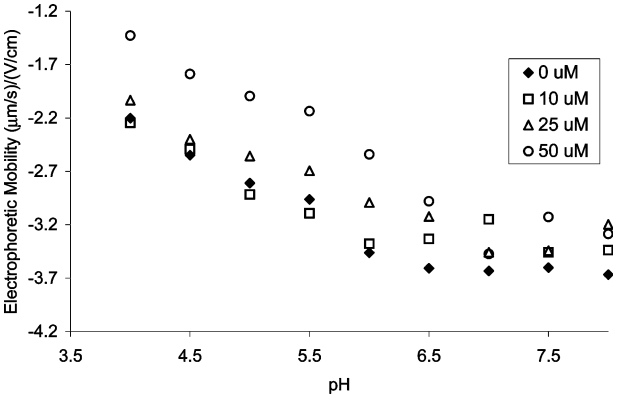

FIGURE 1. Electrophoretic mobility measurements on birnessite as a function of pH and total Zn(II)(aq) concentrations. Reaction conditions: suspension density = 0.1 g L^{-1}, I = 0.01 M NaCl, total Zn(II) concentrations: $[Zn]_T$ = 10−50 μM, and pCO_2=$10^{-3.5}$ atm. Legends indicate total Zn(II) concentrations.

The effects of Zn adsorption on the As(III) oxidation experiments in N_2-purged environments were examined at the same pH values (4.5 and 6.0) in two different systems: (i) As(III) addition to Zn presorbed birnessite and (ii) simultaneous additions of Zn and As(III) to birnessite. In the first system, 100 μM Zn was preadsorbed and equilibrated at pH 4.5 or pH 6.0 for 24 h prior to adding As(III) (100 or 300 μM). In the second system, 100 μM Zn and 100 or 300 μM As(III) were added simultaneously to the system at pH 4.5 and pH 6.0 to simulate environments where the two ions were introduced simultaneously. Samples were taken before As(III) addition (t = 0 min) for total Zn and Mn(II) analyses, and the remaining samples were taken at similar time intervals to those used in the previous experiments. The remaining analyses were as described above, except that the Zn concentration of each sample was determined using ICP-AES.

Results and Discussion

Electrophoretic Mobility Measurements. Figure 1 shows EM values of birnessite suspensions as a function of pH (4−7.5) and different initial Zn concentrations. Electrophoretic mobility measurements indirectly distinguish between inner- and outer-sphere surface complexes on metal oxide particles (*22*). The formation of outer-sphere complexes does not change the EM and IEP of the mineral surface as the adsorbate loading level changes since outer-sphere adsorption occurs at the outer Helmholtz plane (*22*). Inner-sphere complexes shift EM values and the IEP as the loading level increases because of specific ion adsorption inside the shear plane (*22*). When the $[Zn]_T$ concentration increased from 0 to 50 μM, EM values of birnessite particles positively shift with increasing pH. Overall, the EM results indirectly suggest the presence of Zn inner-sphere surface complexes on birnessite surfaces, which agree with a previous study by Loganathan et al. (*23*). Previous extended X-ray absorption fine structure

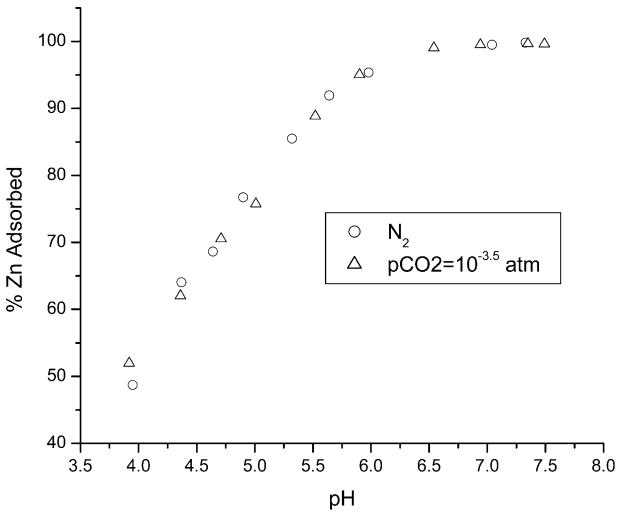

FIGURE 2. pH effects on Zn adsorption on synthetic birnessite (I = 0.01 M NaCl, total Zn(II) concentrations: $[Zn]_T = 100\ \mu M$, and suspension density = 0.1 g L^{-1}) under $pCO_2 = 10^{-3.5}$ and the N_2 atmosphere.

(EXAFS) spectroscopic studies showed Zn formed inner-sphere surface complexes on birnessite surfaces (*27*−*28*).

pH Effects on Zinc Adsorption. Figure 2 shows Zn adsorption on birnessite (birnessite suspension density = 0.1 g L^{-1}, $[Zn]_T = 100\ \mu M$, $I = 0.01$ M NaCl) as a function of pH (4−7.7) and partial pressure of CO_2 (equilibrated in air and N_2). In the air-equilibrated systems, Zn adsorption increased from approximately 50 to 100% (i.e., 2−3 μmol m^{-2}) with increasing pH from 4 to 7 (Figure 2). This pH-dependent adsorption behavior was expected since birnessite became increasingly negatively charged as pH increased above its IEP (1.9). Several researchers reported similar pH-dependent Zn adsorption behavior on birnessite surfaces (*23*−*26*). The Zn adsorption in the N_2 atmosphere showed similar Zn uptake and pH-dependent adsorption behavior. This suggested that dissolved/adsorbed (bi)-carbonate ions did not affect Zn adsorption under the reaction conditions that we studied.

Effects of pH and Initial As(III) Concentration on As(III) Oxidation Kinetics. Figure 3 illustrates the percent As(III) depletion (i.e., As(III) oxidation to As(V)) as a function of time, pH, and initial As(III) concentration. The reaction conditions were abbreviated as As100ph45 ($[As(III)]_i = 100\ \mu M$, pH 4.5), As300ph45 ($[As(III)]_i = 300\ \mu M$, pH 4.5), As100ph6 ($[As(III)]_i = 100\ \mu M$, pH 6.0), and As300ph6 ($[As(III)]_i = 300\ \mu M$ and pH 6.0) in the following discussion. Arsenite readily oxidized to As(V), and the total As adsorption was near negligible after 24 h on the basis of the mass balance calculation of dissolved As(III) and As(V)(aq) for all systems. Scott and Morgan (*6*) reported similar As adsorption on birnessite values upon As(III) oxidation under similar reaction conditions. There were two distinct trends in the As(III) oxidation reactions: (i) the extent of As(III) oxidation decreased with increasing pH from 4.5 to 6.0 and (ii) the extent of As(III) oxidation on a percent basis was suppressed with increasing initial As(III) concentration from 100 to 300 μM.

In the $[As(III)]_i = 100\ \mu M$ systems (Figure 3a,c; Supporting Information Tables 1 and 2), the oxidation reaction was slower at pH 6.0 than at pH 4.5, and approximately 12 h was required to complete the oxidation reaction at pH 6.0 (Figure 3c). The differences in the extent of As(III) oxidation were more pronounced in the $[As(III)]_i = 300\ \mu M$ systems, resulting in slower continuous oxidation reactions even after 24 h at pH 6.0 (Figure 3d). Similar trends were observed in the initial rates, estimated using the initial rate law and dissolved As(V) concentrations at less than 2 h (Table 1). Under excess reactants (i.e., As(III)) at a constant pH, the integrated equation of the initial rate for As(V) production was expressed as

$$\ln[As(V)]_t = k_{obs}t + c \quad (1)$$

where $[As(V)]_t$ = As(V) concentration (mol L^{-1}) at any time t, and k_{obs} = apparent rate coefficient. The apparent rate coefficients for each experiment are shown in Table 1. Although the dissolved As(V) values were slightly underestimated in both 100 μM systems (As100ph45 and As100ph6) because of the small adsorbed fraction during the initial reactions (Figure 3), the rates were consistently higher at pH 4.5 versus 6.0 (k_{obs} (h^{-1}): 7.6 versus 4.7 and 5.4 versus 2.4, respectively) within the same initial As(III)-concentrated systems (Table 1). The time required for half the initial As(III) concentration to disappear from solution (here called $t_{50\%}$) showed a similar trend (Table 1). The value of $t_{50\%}$ was greater at pH 6.0 versus 4.5 ($t_{50\%}$ (h): 1.3 versus 0.6 and 7.0 versus 1.2, respectively) (Table 1). The pH effects on As(III) oxidation could have been influenced by competitive adsorption reactions between As(III) and reaction products (i.e., Mn(II)) and were not influenced by the As(III) solution speciation since dissolved As(III) speciation was identical (i.e., $As(OH)_3^0$) at pH 4.5 and 6.0. The surface charge density of birnessite became more negative with increasing pH and attracted divalent metals, such as Mn(II). The suppressed As(III) oxidation rate constant could be attributed to (i) differences in the amount of Mn(II) release, which competed with dissolved As(III) species for unreacted Mn(IV) surface sites and (ii) Mn(II) adsorption which inhibits the further electron-transfer reactions between As(III)(aq) and unreacted Mn(IV) surface sites. Figure 4a,b shows a comparison between observed and expected Mn(II) release at pH 4.5 and pH 6, respectively. The expected Mn(II) concentrations were estimated via a two-electron-transfer reaction (reaction 1, see below) between As(III) and Mn(IV) (i.e., observed As(V) appearance in Figure 3). At each pH value (Figure 4a,b), it is apparent that (i) the systems at $[As(III)]_i = 300\ \mu M$ produced greater Mn(II) (i.e., observed Mn(II) release) release than in the systems at $[As(III)]_i = 100\ \mu M$ and (ii) the expected Mn(II) release was consistently greater than the observed Mn(II) release (except for As300ph45 at 24 h in Figure 4a, indicating the substantial amount of Mn(II) that could have been adsorbed during the As(III) oxidation. Underestimated expected Mn(II) release (As300ph45 at 24 h) might be attributed to the formation of intermediate products such as $Mn^{III}OOH$(s) that are discussed in the next section. When we compare the effect of pH on Mn(II) adsorption (i.e., the differences between expected and observed Mn(II) release) in the same $[As(III)]_i$ systems, it is greater within the respective reaction condition at pH 6 than at pH 4.5, suggesting Mn(II) adsorption increased with increasing pH from 4.5 to 6. A similar pH-dependent Mn(II) adsorption behavior on birnessite surfaces has been reported by several researchers (*23*, *25*, *29*). Manganese(II) adsorption probably lessened Mn(IV) site availability for dissolved As(III), suppressing As(III) oxidation at pH 6.0. These conclusions were based on macroscopic data and are supported by recent in-situ spectroscopic evidence that showed an increase in surface-bound Mn(II) species upon As(III) oxidation reactions (*8*). On the basis of Figure 4a,b, there was substantial birnessite dissolution which would be associated with changes in the surface areas and properties and may have affected the rate of As(III) oxidation.

Arsenite Oxidation Mechanisms on Synthetic Birnessite. Many researchers investigated As(III) oxidation kinetic reactions by δ-MnO_2, and some observed the overall oxidation reaction (reaction 1). Although the electron-transfer mech-

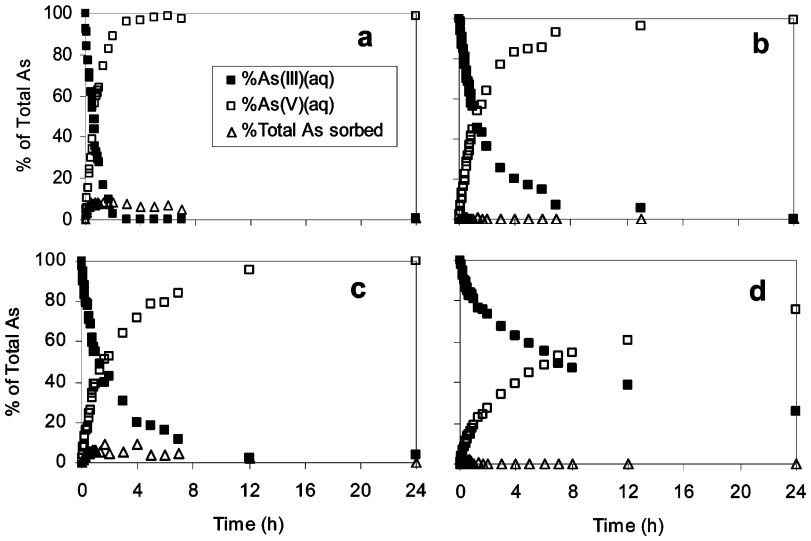

FIGURE 3. Percent of dissolved As(III)(aq), As(V)(aq), and adsorbed As during As(III) oxidation kinetics on birnessite (suspension density = 0.1 g L^{-1}, I = 0.01 M NaCl, and N_2 atmosphere) as a function of pH and initial As(III) concentrations: $[As(III)]_i$. (a) pH 4.5 and $[As(III)]_i$ = 100 μM; (b) pH 4.5 and $[As(III)]_i$ = 300 μM; (c) pH 6.0 and $[As(III)]_i$ = 100 μM; (d) pH 6.0 and $[As(III)]_i$ = 300 μM.

TABLE 1. Apparent Initial Rate Coefficients for As(V) Appearance and Values of $t_{50\%}$ for As(III) Depletion during As(III) Oxidation at the Birnessite−Water Interface

pH	$[Zn(II)]_i$ (μM)	order of Zn(II) addition	$[As(III)]_i$ (μM)	k_{obs}[a] (h^{-1})	$t_{50\%}$[b] (h)
4.5	0	no Zn(II) added	100	7.6	0.6
			300	5.4	1.2
	100	presorbed	100	9.8	3.0
			300	5.7	3.0
		simultaneously added with As(III)	100	7.7	2.0
			300	4.8	2.2
6	0	no Zn(II) added	100	4.7	1.3
			300	2.4	7.0
	100	presorbed	100	NA	12.0
			300	2.3	23.0
		simultaneously added with As(III)	100	2.8	10.5
			300	2.4	22.0

[a] Observed rate coefficients were calculated using pseudo-first-order equations. They were calculated during time intervals where less than 20% of the total As had appeared as As(V) in solution in the systems containing As and birnessite. These time intervals were used to fit pseudo-first-order equations to the systems containing Zn. [b] $t_{50\%}$ is defined as the time for 50% of the initial As(III) concentration to disappear from solution.

anism (i.e., outer- or inner-sphere electron-transfer reactions) has not been demonstrated, experimental evidence suggests that the overall reaction proceeds via two sequential one-electron-transfer steps (*4*, *7*, *30*). First, $Mn^{IV}O_2$ is reduced to form an intermediate reaction product, $Mn^{III}OOH$, and then $Mn^{III}OOH$ is further reacted with As(III) to produce dissolved Mn(II). The formation of $Mn^{III}OOH$ was initially suggested by Hem and Moore (*5*, *30*) and later supported by X-ray photoelectron spectroscopic (XPS) evidence on As(III) reacted birnessite at approximately pH 5.5 (*7*).

$$Mn^{IV}O_2 + H_3AsO_3 + 2H^+ = Mn^{2+} + H_2AsO_4^- + H_2O \quad \text{(reaction 1)}$$

In addition to the $Mn^{III}OOH$ intermediate products in the overall As(III) oxidation step on Mn(IV) oxide surfaces, recent studies indicated the importance of Mn(III) impurities in synthetic δ-MnO_2 upon reacting with Cr(III), sulfide, phenol, and catechol (*7*, *16*, *18*). They showed that Jahn−Teller distorted Mn(III) species in synthetic birnessite was a more reactive oxidant than Mn(IV) (*7*, *16*, *17*). The pyrophosphate

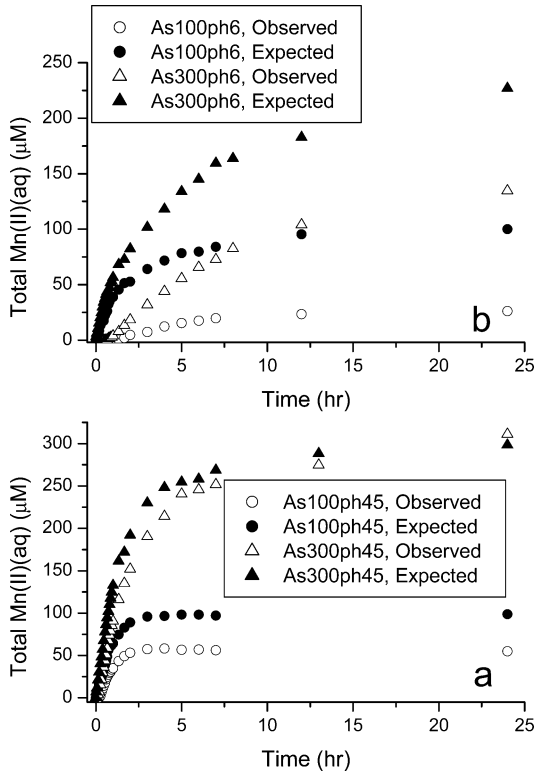

FIGURE 4. (a) Mn(II)(aq) release at pH 4.5 during As(III) oxidation at the birnessite−water interface under the same reaction conditions as Figure 3. As100ph45 (pH 4.5, initial As(III) concentrations: $[As(III)]_i$ = 100 μM); As300ph45 (pH 4.5, $[As(III)]_i$ = 300 μM); (b) Mn(II)(aq) release at pH 6.0 during As(III) oxidation at the birnessite−water interface under the same reaction conditions as Figure 3. As100ph6 (pH 6.0, $[As(III)]_i$ = 100 μM); As300ph6 (pH 6.0, $[As(III)]_i$ = 300 μM). Open symbols: experimentally observed [Mn(II)] release and filled symbols: expected Mn(II) release based on a stoichiometric reaction between Mn(IV) and As(V) (i.e., observed As(V) appearance in Figure 3).

extraction data in this study and previous XPS analyses showed the presence of Mn(III) in synthetic δ-MnO_2 (*7*, *17*). Manganese(III) species are not only structurally incorporated into $Mn^{III}OOH$(s) but surface bound at the layered vacancy sites (*15*, *31*). The dissolved Mn(III) concentrations before/

during the As(III) oxidation were monitored using the method described by Kostka et al. and Matocha (*13*, *32*). Since the dissolved Mn(III) concentrations fluctuated (1−3 μM) near the detection limit during oxidation, it remained inconclusive whether dissolved Mn(III) contributed to the As(III) oxidation.

Other important As(III) oxidation inhibitory processes could have taken place at the birnessite−water interface besides, or in addition to, inhibition via Mn(II) adsorption. They were (i) As(V) adsorption and (ii) the formation of As(V)−Mn(II) precipitates. Figure 3 showed that As (total) was only slightly retained during the initial several hours in the 100 μM As(III) systems (As100ph45 and As100ph6). Although it is difficult to probe As surface speciation at times less than 8 h during the rapid As(III) oxidation reaction, Manning and co-workers used X-ray absorption spectroscopy (XAS) to show the presence of As(V) at the birnessite surface upon As(III) oxidation (*9*). The reaction products were interpreted as bidentate binuclear corner-sharing adsorption complexes with a As(V)−Mn interatomic distance of approximately 3.22 Å. Foster and co-workers reported a bidentate binuclear As(V) adsorption surface species (As(V)−Mn interatomic distance approximately 3.16 Å) upon As(V) reaction with hydrous Mn oxide (*33*). These results indicated that the small fraction of adsorbed As observed at less than 4 h (Figure 3a,c) was probably the As(V) valence state, and the bidentate binuclear As(V) adsorption complexes could have blocked the electron-transfer reaction between As(III)(aq) and Mn(IV) surface sites.

The other inhibitory process that could have occurred was a Mn(II)−As(V) precipitate forming on the birnessite surface. Tournassat and co-workers suggested the formation of krautite-like minerals ($Mn_3(AsO_4)_2$) on As(III)-reacted synthetic birnesite using XAS, scanning transmission microscopy, and energy dispersive spectroscopy and thermodynamic calculations (*8*). The suspension density and initial As(III) concentrations used in this study were much lower (i.e., 0.1 g L^{-1} and $[As(III)]_i = 100-300$ μM) than those used by Tournassat et al. (*8*). Dissolved Mn(II) and As(V) did not contribute to the formation of Mn(II)−As(V) precipitates in these systems. The log(IAP) of $Mn_3(AsO_4)_2$ and $Mn_3(AsO_4)_2 \cdot 8H_2O$ were estimated on the basis of the thermodynamic values reported by Sadiq and MINEQL+ (*21*, *34*), using the dissolved Mn(II) and As(V) concentrations. The estimated log(IAP) values during these experiments were consistently lower than log(K_{sp}) values of these minerals, suggesting the systems were undersaturated with respect to these minerals (Supporting Information Table 3). Therefore, we exclude the possibility that the inhibitory process was due to Mn(II)−As(V) surface precipitates.

Effects of Preadsorbed and Simultaneously Added Zn(II) on As(III) Oxidation Kinetics. Figures 5−7 and Supporting Information Figures 1 and 2 present the aqueous profiles of As(III), As(V), Mn(II), and Zn during the As(III) oxidation kinetics of birnessite in the presence of 100 μM total Zn. Two orders of adding Zn, (i) Zn presorption prior to As(III) addition and (ii) simultaneously added Zn with As(III), were employed to assess the impact of Zn on As(III) oxidation kinetics at the birnessite−water interface. At $t = 0$ min, while 100% Zn was present in solution in the Zn/As(III) simultaneously added systems, approximately 72% (0.14 mg m^{-2}) and 97% (0.19 mg m^{-2}) was retained on the birnessite surfaces in the Zn(II) presorbed systems at pH 4.5 and pH 6.0, respectively. Although adsorbed Zn was present in these systems, As(III) readily oxidized with increasing time (Figure 5). Abbreviations for each reaction condition were used in the following discussion and in Figures 5−7. For example, "PAs100ph45" was for the 100 μM of Zn presorbed prior to the 100 μM As(III) addition at pH 4.5 and "SAs100ph6"

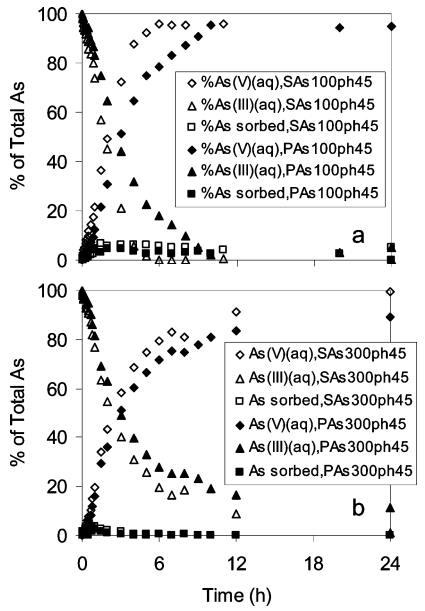

FIGURE 5. Effects of presorbed Zn(II) vs Zn(II)/As(III)-simultaneous treatment on the As(III) oxidation kinetics on birnessite surfaces (pH 4.5, suspension density = 0.1 g L^{-1}, I = 0.01 M NaCl, total Zn(II) concentrations: $[Zn(II)]_T$ = 100 μM, and N_2 atmosphere). Percent As(III) depletion, As(V) release, and total As adsorption are shown as a function of time (h). (a) initial As(III) concentrations: $[As(III)]_i$ = 100 μM; (b) $[As(III)]_i$ = 300 μM.

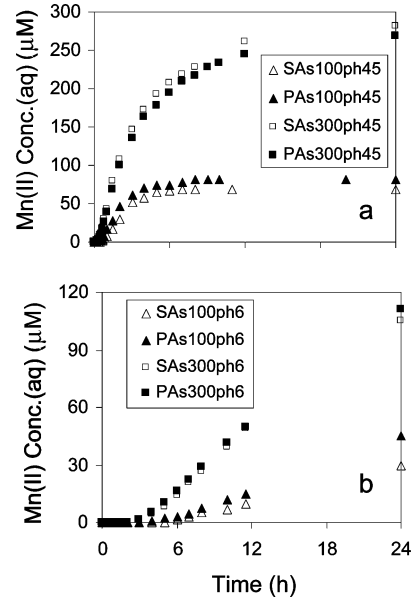

FIGURE 6. Effects of presorbed Zn(II) vs Zn(II)/As(III)-simultaneous treatment on the Mn(II) release during the As(III) oxidation kinetics on birnessite surfaces (suspension density = 0.1 g L^{-1}, I = 0.01 M NaCl, total Zn(II) concentrations: $[Zn]_T$ = 100 μM, and N_2 atmosphere). (a) initial As(III) concentrations: $[As(III)]_i$ = 100 and 300 μM at pH 4.5; (b) $[As(III)]_i$ = 100 and 300 μM at pH 6.

was for the simultaneous 100 μM Zn/100 μM As(III) addition at pH 6.0.

The effects of the different Zn addition orders on As(III) oxidation at pH 4.5 and 6.0 were compared. In the systems containing Zn at pH 4.5 (Figure 5, Supporting Information Tables 1 and 2), the extent of As(III) oxidation was more suppressed in the Zn presorbed system than the simultaneous Zn/As(III) added systems. In both systems containing Zn (Figure 5), As(III) oxidation was nearly complete after 24 h, except for PAs300ph45. A similar trend was seen in the $t_{50\%}$

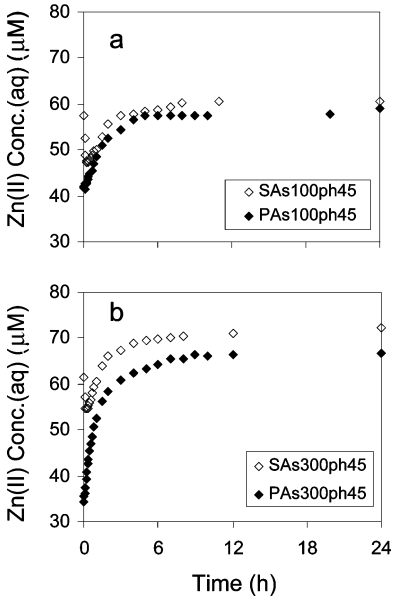

FIGURE 7. Effects of the presorbed Zn(II) vs Zn(II)/As(III)-simultaneous treatment on the aqueous profiles of Zn during the As(III) oxidation kinetics on birnessite surfaces (pH 4.5, suspension density = 0.1 g L^{-1}, I = 0.01 M NaCl, total Zn(II) concentration: $[Zn]_T$ = 100 μM, and N_2 atmosphere). (a) initial As(III) concentrations: $[As(III)]_i$ = 100 μM; (b) $[As(III)]_i$ = 300 μM.

values (Table 1). Both presorbed systems (i.e., PAs100ph45 and PAs300ph45) had $t_{50\%}$ = 3 h, and the half-life values in the simultaneously added systems were higher in SAs300ph45 than SAs100ph45 (i.e., 2.2 vs 2.0 h, respectively). Electrophoretic mobility measurements and XAS evidence from other researchers (*27*, *28*) indicated Zn was likely to form inner-sphere complexes on birnessite surfaces as well as on $Mn^{III}OOH$(s) (*35*). Chemisorbed Zn ions probably inhibited the electron-transfer reaction. Manganese(II) adsorption could have out-competed Zn for adsorption sites since the aqueous Mn(II) concentration was consistently higher than the aqueous Zn concentration throughout the experiments (Figures 6 and 7). Zinc in the Zn/As(III) simultaneously added systems (SAs100ph45 and SAs300ph45) was rapidly adsorbed initially, but the release of Zn continued with increasing time in both presorbed and simultaneously added systems at pH 4.5 (Figure 7), suggesting (i) competitive Mn(II) adsorption reactions or (ii) surface alternation due to the reductive dissolution of birnessite.

In the systems containing Zn at pH 6.0 (Supporting Information Figure 1), the Zn presorbed systems suppressed As(III) oxidation more than the Zn(II)/As(III) simultaneously added systems. A biphasic reaction for As(V) release was observed in the systems containing Zn at pH 4.5, with the extent of As(V) release at pH 6.0 much slower and nearly linear (Supporting Information Figure 1), resulting in an incomplete As(III) oxidation after 24 h. The trend was also observed in the $t_{50\%}$ values (Table 1). This study suggested the differences in oxidation among the two initial As(III) concentrations were due to pH-dependent metal adsorption behavior. Dissolved Mn(II) and Zn concentrations were significantly lower at pH 6.0 than at pH 4.5 with increasing time (Supporting Information Figures 1 and 2), suggesting enhanced divalent metal uptake.

The formation of Mn(II)/Zn(II)−As(V) precipitates ($Mn_3(AsO_4)_2$, $Mn_3(AsO_4)_2{\cdot}8H_2O$, $Zn_3(AsO_4)_2$, $Zn_3(AsO_4)_2{\cdot}5H_2O$) on the birnessite surfaces could also inhibit/suppress electron-transfer reactions. A similar concept was experimentally proven by Oscarson and co-workers who showed that aluminum oxide/calcite coatings on birnessite surfaces effectively suppressed As(III) oxidation (*4*). The dissolved Mn(II), As(V), and Zn concentrations in this study were used to estimate log(IAP) values. The log(IAP) values for each solid, at any time in each system, were significantly lower than the log(K_{sp}) values, suggesting all pH 4.5 and 6.0 systems were undersaturated with respect to manganese arsenate and zinc arsenate precipitates (Supporting Information Table 3).

When $t_{50\%}$ values were compared within the initial As(III)-concentrated systems (100 or 300 μM) (Table 1), the Zn presorbed systems suppressed As(III) oxidation the most at each pH (3 h for PAs100/300ph45, 12 h for PAs100ph6, 23 h for PAs300ph6). The Zn and As(III) simultaneous addition increased the half-lives, but not as much as the presorbed Zn systems. The $t_{50\%}$ values were 2−3 times greater at pH 4.5 and more than tripled at pH 6.0 when the Zn was presorbed verses simultaneously added with As(III).

The highest $t_{50\%}$ values were in the Zn presorbed systems at the same pH (3 h for PAs100/300ph45 and 23 h for PAs300ph6). The presence of Zn diminished the effects of aqueous initial As(III) concentration on the half-life at pH 4.5, resulting in the near equal half-lives (i.e., 3 h for the presorbed, and 2−2.2 h for the simultaneously added systems). Divalent Zn suppression on As(III) oxidation was summarized in the As(III)(aq) profile during the oxidation reactions (Supporting Information Tables 1 and 2). Presorbed and nonadsorbed (i.e., as dissolved competitive ligands) Zn played an important role in suppressing As(III) oxidation on birnessite surfaces during the intermediate reaction times.

The effects of adsorbed and nonadsorbed Zn on As(III) oxidation were observed during the initial reactions. The k_{obs} values for the Zn presorbed and simultaneously added systems were generally lower than that of their respective controls, systems containing As(III) without Zn (Table 1), indicating As(III) oxidation was suppressed in most of the systems containing Zn. During intermediate reaction times, Zn presorption suppressed the As(III) oxidation reaction the most compared to the respective control systems. The initial hypothesis in this study that Zn inner-sphere complexation on the birnessite surface would interfere with As(III)/Mn(IV) redox reactions could be applied to most of the reaction conditions. This interference suppressed As(III) oxidation at the initial and intermediate reaction times, except for in one system. At the initial time (<20 min) for the PAs100ph45 and PAs300ph45 systems, inner-sphere Zn adsorption enhanced initial As(III) oxidation. The k_{obs} values for As(V) release were higher in these Zn presorbed systems (9.8 and 5.7 h^{-1}) (Table 1).

The results of this study showed that the extent and rate of As(III) oxidation on birnessite surfaces were highly influenced by sorbed or competitive metal ligands in solutions (e.g., Mn(II) and Zn). An increase in the initial As(III) concentrations or pH suppressed As(III) oxidation which was presumably due to the adsorption of Mn(II) that was readily produced as reaction products. When Zn was present, As(III) oxidation was further suppressed by nonadsorbed and presorbed Zn compared to the respective control systems. Nonadsorbed Zn had a competitive effect to reduce the oxidation rate, and inner-sphere Zn adsorption that occurred in the Zn presorbed systems was more effective in interfering with electron-transfer reactions. These findings are useful in further understanding the potential As(III) oxidation in natural systems containing manganese oxide and competing metal ligands.

Acknowledgments

We thank Dr. M. Eick (Virginia Polytechnic Institute and State University) for providing access to and assisting with the Zeta Potential Meter and T. Luxton for technical support. We thank Dr. B. McCandless (Institute of Energy Conversion,

University of Delaware) for providing access and assistance to the XRD unit. Thanks are extended to Dr. M. Gräfe (University of Delaware) for his critical comments and to the Associate Editor and the reviewers for their excellent suggestions for improvement of the manuscript.

Supporting Information Available

Three tables and two figures. This material is available free of charge via the Internet at http://pubs.acs.org.

Literature Cited

(1) Tamaki, S.; Frankenberger, W. T., Jr. Environmental biochemistry of arsenic. *Rev. Environ. Contam. Toxicol.* **1992**, *124*, 79−110.

(2) *EPA To Implement 10ppb Standard for Arsenic in Drinking Water;* United States Environmental Protection Agency, 2001; http://www.epa.gov/ OGWDW/ars/ars-oct-factsheet.html.

(3) *Handbook of Chemistry and Physics*, 82nd ed.; Lide, Ed.; Chemical Rubber Company: Boca Raton, FL, 2001.

(4) Oscarson, D. W.; Huang, P. M.; Liaw, W. K.; Hammer, U. T. Kinetics of oxidation of arsenite by various manganese dioxides. *Soil Sci. Soc. Am. J.* **1983**, *47*, 644−648.

(5) Moore, J. N.; Walker, J. R.; Hayes, T. H. Reaction scheme for the oxidation of As(III) to As(V) by birnessite. *Clays Clay Miner.* **1990**, *38* (5), 549−555.

(6) Scott, M. J.; Morgan, J. J. Reactions at oxide surfaces. 1. Oxidation of As(III) by synthetic birnessite. *Environ. Sci. Technol.* **1995**, *29*, 1898−1905.

(7) Nesbitt, H. W.; Canning, G. W.; Bancroft, G. M. XPS study of reductive dissolution of 7 Å birnessite by H_3AsO_3, with contraints on reaction mechanism. *Geochim. Cosmochim. Acta* **1998**, *62*, 2097−2110.

(8) Tournassat, C.; Charlet, L.; Bosbach, D.; Manceau, A. Arsenic(III) oxidation by birnessite and precipitation of manganese(II) arsenate. *Environ. Sci. Technol.* **2002**, *36*, 493−500.

(9) Manning, B. A.; Fendorf, S. E.; Bostick, B.; Suarez, D. L. Arsenic(III) oxidation and arsenic(V) adsorption reactions on synthetic birnessite. *Environ. Sci. Technol.* **2002**, *36*, 976−981.

(10) McKenzie, R. M. The synthesis of birnessite, cryptomelane, and some other oxides and hydroxides of manganese. *Mineral. Mag.* **1971**, *38*, 493−502.

(11) Diebler, H.; Sutin, N. The kinetics of some oxidation−reduction reactions involving manganese(III). *J. Phys. Chem.* **1964**, *68*, 174−180.

(12) Davies, G. Some aspects of the chemistry of manganese(III) in aqueous solution. *Coord. Chem. Rev.* **1969**, *4*, 199−224.

(13) Kostka, J. E.; Luther, G. W., III; Nealson, K. H. Chemical and biological reduction of Mn(III)−pyrophosphate complexes: Potential importance of dissolved Mn(III) as an environmental oxidant. *Geochim. Cosmochim. Acta* **1995**, *59*, 885−894.

(14) Drits, V. A.; Silvester, E.; Gorshkov, A. I.; Manceau, A. Structure of synthetic monoclinic Na-rich birnessite and hexagonal birnessite: I. Results from X-ray diffraction and selected-area electron diffraction. *Am. Mineral.* **1997**, *82*, 946−961.

(15) Silvester, E.; Manceau, A.; Drits, V. A. Structure of synthetic monoclinic Na-rich birnessite and hexagonal birnessite: II. Results from chemical studies and EXAFS spectroscopy. *Am. Mineral.* **1997**, *82*, 962−978.

(16) Nico, P. S.; Zasoski, R. J. Importance of Mn(III) availability on the rate of Cr(III) oxidation on δ-MnO_2. *Environ. Sci. Technol.* **2000**, *34*, 3363−3367.

(17) Matocha, C. J.; Sparks, D. L.; Amonette, J. E.; Kukkadapu, R. K. Kinetics and mechanism of birnessite reduction by catechol. *Soil Sci. Soc. Am. J.* **2001**, *65*, 58−66.

(18) Matocha, C. J. Ph.D. Thesis, University of Delaware, Newark, DE, 2000.

(19) Cummings, D. E.; Caccavo, F., Jr.; Fendorf, S.; Rosenzweig, R. F. Arsenic mobilization by the dissimilatory Fe(III)-reducing bacterium *Shewanella alga* BrY. *Environ. Sci. Technol.* **1999**, *33*, 723−729.

(20) Hiemenz, P. C.; Rajagopalan, R. *Electrophoresis and Other Electrokinetics Phenomena*; Dekker: New York, 1997.

(21) Schecher, W. D.; McAvoy, D. C. *MINEQL+*; Environmental Research Software: 1998.

(22) Hunter, R. J. *Colloid Science, A Series of Monographs*; Academic Press: San Diego, CA, 1981; p 219.

(23) Loganathan, P.; Burau, R. G.; Fuerstenau, D. W. Influence of pH on the sorption of Co^{2+}, Zn^{2+} and Ca^{2+} by a hydrous manganese oxide. *Soil Sci. Soc. Am. J.* **1977**, *41*, 57−62.

(24) Loganathan, P.; Burau, R. G. Sorption of heavy metal ions by a hydrous manganese oxide. *Geochim. Cosmochim. Acta* **1973**, *37*, 1277−1293.

(25) Murray, J. W. The interaction of metal ions at the manganese dioxide-solution interface. *Geochim. Cosmochim. Acta* **1975**, *39*, 505−519.

(26) Zasoski, R. J.; Burau, R. G. Sorption and sorptive interaction of cadmium and zinc on hydrous manganese oxides. *Soil Sci. Soc. Am. J.* **1988**, *52*, 81−87.

(27) Manceau, A.; Lanson, B.; Drits, V. A. Structure of heavy metal sorbed birnessite. Part III. Results from powder and polarized extended X-ray absorption fine structure spectroscopy. *Geochim. Cosmochim. Acta* **2002**, *66*, 2639−2663.

(28) Roberts, D. R.; Scheinost, A. C.; Sparks, D. L. Zn speciation in a smelter-contaminated soil profile using bulk and microspectroscopic techniques. *Environ. Sci. Technol.* **2002**, *36*, 1742−1750.

(29) Stone, A. T.; Ulrich, H.-J. Kinetics and reaction stoichiometry in the reductive dissolution of Mn(III,IV) and Co(III) oxides by hydroquinone. *J. Colloid Interface Sci.* **1989**, *132*, 509−522.

(30) Hem, J. D. Redox processes at surfaces of manganese oxide and their effects on aqueous metal ions. *Chem. Geol.* **1979**, *21*, 199−218.

(31) Nico, P. S.; Zasoski, R. J. Mn(III) center availability as a rate controlling factor in the oxidation of phenol and sulfide on δ-MnO_2. *Environ. Sci. Technol.* **2001**, *35*, 3338−3343.

(32) Matocha, C. J. University of Kentucky, Lexington, KY, Personal communication, 2003.

(33) Foster, A. L.; Brown, G. E., Jr.; Parks, G. A. XAFS study of As(V) and Se(IV) sorption complexes on hydrous Mn oxides. *Geochim. Cosmochim. Acta* **2003**, *67*, 1937−1953.

(34) Sadiq, M. Arsenic Chemistry in Soils: An overview of thermodynamic predictions and field observations. *Water, Air, Soil Pollut.* **1997**, *93*, 117−136.

(35) Bochatay, L.; Persson P. Metal ion coordination at the water−manganite (γ-MnOOH) interface. II. An EXAFS study of zinc(II). *J. Colloid Interface Sci.* **2000**, *229*, 593−599.

Received for review January 15, 2004. Revised manuscript received October 11, 2004. Accepted October 14, 2004.

ES049922I